Environmental Science Nano



PAPER

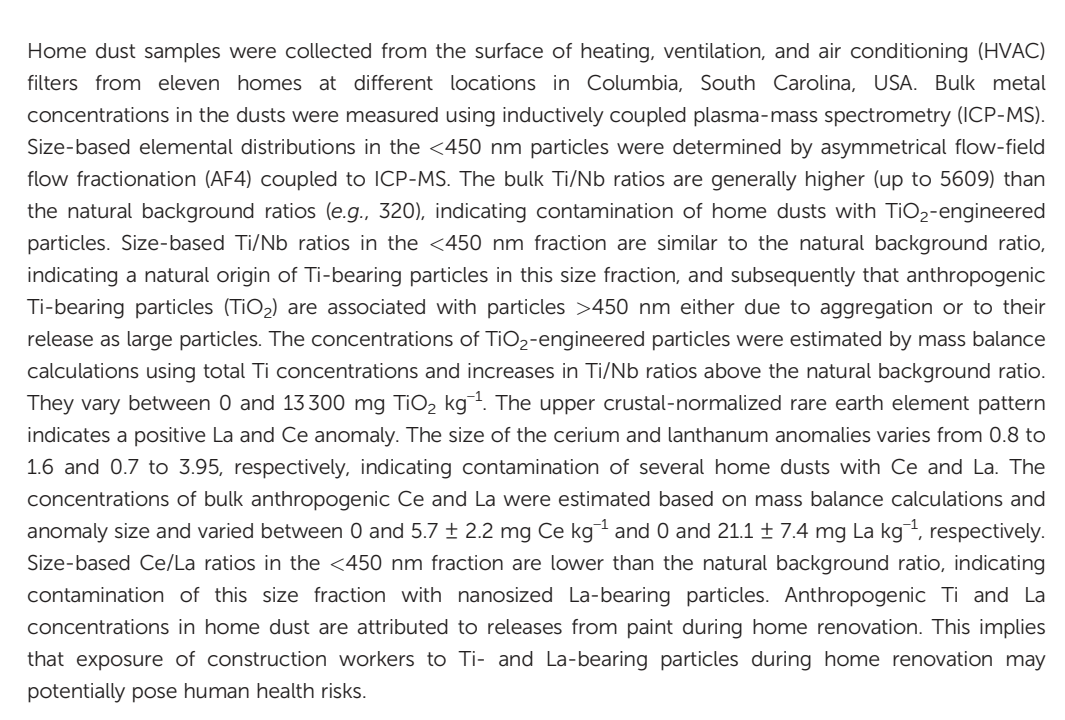
View Article Online



Cite this: DOI: 10.1039/d2en00890d

Detection and quantification of anthropogenic titanium-, cerium-, and lanthanum-bearing home dust particles†

Md Mahmudun Nabi, Jingjing Wang and Mohammed Baalousha 10 *



Received 27th September 2022, Accepted 10th March 2023

DOI: 10.1039/d2en00890d

rsc.li/es-nano

Environmental significance

Engineered particles are widely found in the indoor environment; however, there are currently no data on their concentrations in home dusts. Therefore, this study investigated the concentrations and size distributions of Ti-, Ce-, and La-bearing particles in home dusts collected from the surface of heating, ventilation, and air conditioning (HVAC) filters. The anthropogenic concentrations of Ti, Ce, and La vary between 0 and 8000, 0 and 6, and 0 and 21 mg kg⁻¹, respectively. Whereas Ti occurs predominantly as part of large fragments, La occurs predominantly as nanosized particles. Anthropogenic Ti, Ce, and La concentrations in home dust are attributed to release from paint, in particular during home renovation. The findings of this study imply that exposure of construction workers and residents to Ti-, Ce-, and La-bearing particles, in particular during home renovation, may potentially pose human health risks.

1. Introduction

Human exposure to indoor contaminants is an emerging area of health concern, especially because people spend up to 90% of their time indoors.^{1–3} In developed countries, people spend

Center for Environmental Nanoscience and Risk, Department of Environmental Health Sciences, Arnold School of Public Health, University of South Carolina, Columbia, South Carolina, USA. E-mail: mbaalous@mailbox.sc.edu

† Electronic supplementary information (ESI) available. See DOI: https://doi.org/10.1039/d2en00890d

approximately 65% of their daily time at home, with the young and elderly spending even more time at home. 4,5 Indoor dust accumulates environmental contaminants over extended periods and thus has the potential to be used for retrospective exposure assessment. Many studies have investigated indoor dust to detect human exposure to a variety of chemical, physical, biological, and radiological contaminants. Indoor dust is a complex mixture of particulate matter derived from a range of indoor and outdoor sources, which acts as both a sink and a transport medium for contaminants such as metals and nanomaterials. Indoor sources of particles include paint,

renovation, cooking, indoor combustion, smoking, vaping, secondary formation processes, and dust resuspension.8-14 Outdoor (atmospheric) particles in the urban environment originate predominantly not only from fossil fuel burning, automobile emissions, resuspension, or chemical and thermodynamic processes but also from long-range transport.15

Several studies determined the concentrations of metals in home dust/particulate matter (PM).16 However, information on the occurrence and concentrations of metalbearing nanomaterials in home dust remains scarce. 14,17,18 Several studies have investigated bulk metal concentrations in the fine and submicron fractions of indoor PM. 19,20 Bari et al. identified dust resuspended from carpets as a source of Sb, electrical appliances as a source of Cu, and consumer products as a source of Ag in very fine particulate matter (PM₁ <1 μm) in homes.¹⁹ Suryawanshi *et al.* identified wall dust (i.e., coatings and building materials) as a major source of indoor metal pollution and as a source of Ca, Cu, Fe, Pb, Mg and Ni in particulate matter <0.6 µm (PM_{0.6}).²⁰ Other studies investigated particulate matter composition at the single-particle level using electron microscopy and energydispersive X-ray spectroscopy. 17,18 Conner et al. identified cosmetics and personal care products as a possible source of several elements in indoor particulate matter (PM_{2.5} <2.5 μm), including Al, Bi, Ti, Mg, Si and Fe.¹⁷ Calderón et al. identified consumer spray products as a source of nanoscale (<100 nm) and coarse aerosol particles (>2.5 µm) containing Ag, Zn, Li, Sr, Ba, Pb, Mn, and other elements. 18 Other studies, using X-ray microanalysis, demonstrated that metals accumulate in house dust from common building materials and products such as Pb solder, As- and Cr-treated wood, and paint pigments containing Zn, Ti, Cr, Pb and Ba. 14,21-24

The detection of anthropogenic particles in environmental samples is complicated by the similarity of their physicochemical properties, such as size, shape, and elemental composition, to those of natural particles. 25,26 Thus, analytical approaches are being developed to differentiate natural from anthropogenic particles.^{25,27–29} These approaches include bulk elemental ratio analysis (e.g., Ce/La (ref. 25, 30 and 31) and Ti/ Nb (ref. 32-37)), size-based elemental ratio analysis, 38,39 singleparticle elemental fingerprinting,40-43 and morphological analysis using electron microscopy. 34,38,44 For instance, singleparticle elemental fingerprinting by single-particle inductively coupled plasma mass spectrometry (SP-ICP-MS) is limited by the minimal detectable masses, which are element dependent.45 Thus, nanomaterials with masses smaller than the minimal detectable masses cannot be characterized by SP-ICP-MS. Additionally, it is not possible to differentiate a true single-element particle from a multi-element particle containing natural tracers with concentrations smaller than the minimal detectable mass using multi-element single-particle analysis.46 Morphological analysis of nanomaterials, typically performed using transmission electron microscopy (TEM), suffers from poor statistical power due to the limited number of particles that can be imaged and analyzed within a

reasonable time and cost frame. 47,48 The bulk- and size-based elemental ratio approach can be hampered by cocontamination with the element of interest and the reference element (e.g., co-contamination with Ce and La). In the case of co-contamination with rare earth elements (REEs), another approach that can be applied to differentiating natural from anthropogenic REEs is the normalization of REE concentrations to the upper crustal concentrations and the determination of REE anomalies. 49,50 Normalization of REE concentrations in a given sample to the corresponding upper crustal REE concentrations removes the natural variations in absolute REE concentrations, resulting in a smooth REE pattern. Perturbations/spikes in the normalized REE concentration profile allow the identification of enrichment with a given REE.

The aims of this study are to (1) determine anthropogenic Ti, Ce, and La concentrations in home dust and (2) determine the particle size distribution of anthropogenic Ti, Ce, and La in home dust. To this end, home dusts were collected from the surface of heating, ventilation, and air conditioning (HVAC) filters from eleven homes at different locations in Columbia, South Carolina, USA. Home dusts were analyzed for bulk metal concentrations following digestion by inductively coupled plasma-mass spectrometry (ICP-MS) and size-based elemental distributions by asymmetrical flow-field flow fractionation (AF4) coupled to ICP-MS, from which bulk and size-based elemental ratios determined. Anthropogenic elemental/particle were concentrations were determined by mass balance calculations and shifts in elemental ratios above the natural background ratios and the size of REE anomalies.

2. Materials and methods

2.1. Sampling and analysis

Dust samples were collected from the surface of HVAC filters from eleven different homes in Columbia, SC (Fig. S1†). Dust samples were gently scraped from the surface filters and placed in a 50 mL acid-washed test tube, which was sealed in a ziplock bag, labeled and returned to the laboratory. No information was available about the type of the filters used in these homes. Therefore, five different HVAC filters were purchased as a potentially representative group of HVAC filters used in homes including basic pleated (BP), advanced allergen (AA), microparticle reduction (MR), allergen reduction (AR), and dust reduction (DA) air filters. These filters were used as blanks to measure metal concentrations in clean/unused HVAC filters. Small pieces (ca. 1 cm \times 1 cm) of the HVAC filters were cut using a pair of clean ceramic scissors, placed inside airtight Teflon vessels (Savillex, Eden Prairie, MN, USA), and then digested according to the same procedure used for the digestion of the dust samples.

2.2. Sample digestion and elemental analysis

Dust samples were fully digested using a mixture of reagents, including H₂O₂, HNO₃, and HF, using a modified method

Published on 13 March 2023. Downloaded by University of South Carolina Libraries on 3/29/2023 2:01:34 PM.

from our previous study.⁵¹ Due to the high organic content, 25 or 50 mg dust samples were treated with 1 mL of 30% H₂O₂ (Fisher Chemical, Fair Lawn, NJ, USA) at 70 °C, then completely dried at 110 °C. The process was repeated twice to fully remove organic matter. Then, the residue was digested using a distilled HF: HNO₃ (1:3) mixture (ACS-grade acids distilled in the laboratory, Sigma Aldrich, St. Louis, MO, USA) at 110 °C for 48 h. Additional distilled HNO3 was added to the samples to break down any insoluble fluoride salts. At the end of the digestion procedure, the samples were transferred to acid-prewashed centrifuge tubes using 1% trace metal grade HNO3. Clean/unused HVAC filter pieces were also digested following the same procedure described above to determine the metal content in the HVAC filters themselves. USGS reference material BHVO-2 Hawaiian basalts was digested using the same procedure to verify the method accuracy. All digested samples were stored at 4 °C before analysis.

Elemental concentrations were measured using a Perkin Elmer NexION 350D ICP-MS instrument (Perkin Elmer, Waltham, MA, USA) after a routine standard tuning procedure. Instrument operating parameters are listed in Table S1.† The monitored isotopes are listed in Table S2.† Calibration curves for the monitored isotopes were established by measuring a series of ICP standards (BDH Chemicals, Radnor, PA, USA) with concentrations ranging from 0.01 to 1000 mg L⁻¹. Internal standards (5 µg L⁻¹ Li, Sc, Y, In, Tb, and Bi in 1% HNO₃, ICP Internal Element Group Calibration Standard, BDH Chemicals, Radnor, PA, USA) were measured as independent samples after each water sample to monitor any signal drift. No drift was observed for the internal standards throughout the analysis time. All data were collected using Syngistix 1.0 software. Elemental analysis of digested USGS reference material BHVO-2 demonstrated the high recovery, accuracy, and precision for most elements (Table S2†), confirming the reliability of the method.

2.3. Nanomaterial extraction and size distribution

The <450 nm size fraction was extracted from the home dusts following the procedure described in detail in our previous study.⁵¹ Briefly, dusts were suspended in 10 mM tetrasodium pyrophosphate at pH 10 for 24 h by overhead 360-degree rotation. Then, the <450 nm size fraction was separated by centrifugation (Eppendorf, 5810 R, Hamburg, Germany) at 775g for 25 min (<450 nm assuming natural particle density $\rho = 2.5 \text{ g cm}^{-3}$) to prevent clogging of the ICP-MS introduction system.

The extracted suspensions were fractionated based on the particle diffusion coefficient, and thus equivalent spherical hydrodynamic diameter, using Wyatt Eclipse DualTec asymmetrical flow-field flow fractionation (AF4, Wyatt Technology Corporation, Santa Barbara, CA, USA). The AF4 channel characteristics and fractionation parameters are summarized in Table S3.† The AF4 carrier phase consists of 10 mM NaNO₃, 0.0125% FL-70 surfactant, and 0.01% NaN₃, a

typical carrier phase used for the fractionation of natural and engineered nanomaterials.52,53 The 10 mM NaNO3 is used to partially screen the AF membrane surface charge, without inducing nanomaterial aggregation, and thus to minimize the impact of membrane-nanomaterial electrostatic interactions on nanomaterial separation. The FL-70 surfactant is used to prevent/minimize nanomaterial aggregation. NaN3 is used to prevent any potential biological growth in the AF4 channel. The elemental concentrations of the fractionated particles were then measured via online ICP-MS. Prior to sample analysis, both AF4 and ICP-MS were tuned and calibrated separately. A Y-connector (PEEK, Analytical Sales & Services, Flanders, NJ, USA) was used to mix the AF4 effluent or the ICP-MS calibration standard (prepared in the AF4 carrier phase) with the internal standard (5 $\mu g L^{-1} Li$, Sc, Y, In, Tb, and Bi in 2% HNO₃) at a 1:1 (v:v) ratio and to transport the mixture into the ICP-MS. In order to eliminate carry-over, a 20 min 1% HNO3 (Trace Metal Grade, Fisher Chemical, Fair Lawn, NJ, USA) rinse followed by a 10 min UPW rinse was applied between samples. AF4-ICP-MS data were collected using Chromera 4.1.0.6386 software.

2.4. Estimation of anthropogenic Ti concentration

The concentration of anthropogenic Ti was estimated based on mass balance calculations according to eqn (1)

$$\text{Anthropogenic Ti} = \left[\text{Ti}_{\text{dust}} - \text{Nb}_{\text{dust}} \cdot \left(\frac{\text{Ti}}{\text{Nb}} \right)_{\text{background}} \right]$$
 (1)

where Ti_{dust} and Nb_{dust} are the concentrations of Ti and Nb in a given dust sample, and Ti/Nb_{background} is the natural background elemental concentration ratio of Ti/Nb. Here, we used the average crustal Ti/Nb of 320 as the natural background ratio.54

2.5. Rare earth element anomalies and estimation of anthropogenic Ce and La concentrations

Shale normalized REE concentration (REE $_n$) patterns are a representation of the measured concentrations of REEs in a given sample divided by their respective concentrations in a reference shale plotted against atomic number. Here, we normalized the REE concentrations in the home dusts to the average upper crustal REE concentrations reported by Rudnick et al.54 For uncontaminated samples, the crustalnormalized REE patterns are smooth. In contrast, the crustalnormalized REE patterns exhibit anomalous increases/ decreases relative to the overall pattern for REEs with anthropogenic contributions.

Determining the size of the REE anomaly (REE_n/REE_n^*) in contaminated samples can be complicated by sample cocontamination with several neighboring REEs. The principal requirement for calculating REE anomalies is that the near neighbors used in the calculations must not show any anomalous behavior themselves. For example, for the calculation of La* we cannot use Cen, as contamination with Ce will affect the calculation of La* and vice versa. As a result,

La and Ce anomalies were calculated using nearest available non-anomalous REEs (e.g., Pr_n and Nd_n) according to eqn (2) and (3).55

$$La^* = Pr_n^* (Pr_n/Nd_n)^2$$
 (2)

$$Ce^* = \Pr_n^*(\Pr_n/Nd_n)$$
 (3)

The anthropogenic REE concentration (REEAnth) is then calculated using eqn (4):⁵⁶

$$[REE_{Anth}] = \frac{\left(\frac{REE}{REE_n^*} - 1\right)}{\left(\frac{REE}{REE_n^*}\right)} \times [REE_{measured}]$$
(4)

where $[\text{REE}_{\text{Measured}}]$ is the measured REE concentration in the dust samples.

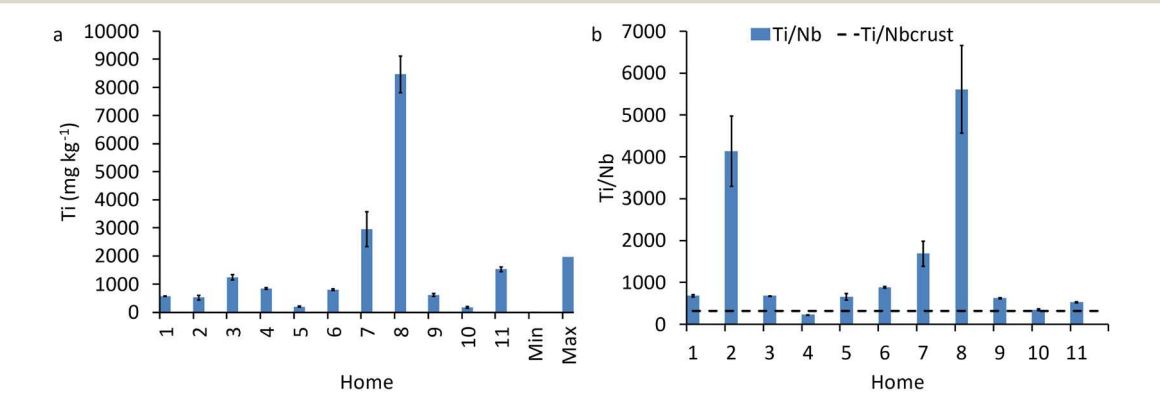
3. Results and discussion

3.1. Metals in house dust

The concentrations of the 34 elements measured in the eleven home dusts are presented in Fig. S2.† Overall, Al, Fe, Ti, and Mn display the highest concentrations in all dusts and their concentration varies from a few mg kg⁻¹ to several thousands of mg kg⁻¹ (Fig. S2a†). The

concentrations of Zn, Zr, Cu, and Ba vary from a few mg kg⁻¹ to several hundreds of mg kg⁻¹ (Fig. S2b†). The concentrations of Sr, Cr, Ni, Pb, V, Mo, Hf, and Co vary from sub-mg kg⁻¹ to several tens of mg kg⁻¹ (Fig. S2c†). The concentrations of Nb, Th and Ta vary from sub-mg kg⁻¹ to a few mg kg⁻¹ (Fig. S2d†). The concentrations of REEs vary from sub-mg kg⁻¹ to a few tens of mg kg⁻¹ (Fig. S2e and f†). These elements could originate from natural sources such as soil particles or from anthropogenic sources such as road dust, or releases from building materials, appliances, and furniture. 57-60

Different home dusts are characterized by high concentrations of certain elements (Fig. S2†). For instance, dust from home 4 is characterized by higher Mn, Cr, Ni, V, Mo, and Co concentrations than all other dust samples. Dust from home 8 is characterized by higher Ti, Sr, Ce, and La concentrations than all other dust samples. Dust from home 7 is characterized by higher Ti and Pb than all other dust samples. Dust from home 11 is characterized by higher concentrations of Al, Fe, Zn, Cu, Ba, Ni, V, Pb, Nb, Th, and all the REEs than all other dust samples. Below, we focus on a few of these elements including Ti, Ce, and La, and we attempt to differentiate natural from anthropogenic sources of these elements and estimate their concentrations using mass balance calculations.



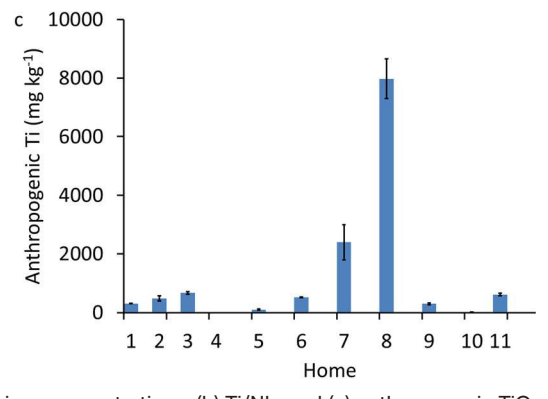


Fig. 1 (a) Titanium concentrations, (b) Ti/Nb, and (c) anthropogenic TiO₂ concentrations in bulk home dusts collected from the surface of heating, ventilation, and air conditioning (HVAC) units from residential homes. Min and max refer to the minimum and maximum Ti concentrations detected in the five black HVAC filters. Concentrations are presented as mean \pm standard deviation of three replicates.

3.2. Anthropogenic titanium concentrations

The concentrations of Ti in home dusts vary between 161 \pm 32 and 8464 \pm 660 mg kg⁻¹ (Fig. 1a). The Ti concentrations measured in the current study are higher than those reported (e.g., $2000 \pm 995 \text{ mg kg}^{-1}$) in home dust in Christchurch, New Zealand, 61 and Jersey City, New Jersey, USA, households (e.g., $1060 \pm 160 \text{ mg kg}^{-1}$ to $1640 \pm 245 \text{ mg kg}^{-1}$). 62 However, it is worth noting that the Ti concentration in some of the blank filters was also high and ranges from 0.7 \pm 0.6 to 1952 \pm 283 mg kg⁻¹. Nonetheless, the Ti concentrations in home dust 7 and 8 are respectively 1.5- and 5-fold higher than the highest Ti concentration in the five blank filters. The concentration of Ti in all other home dusts was lower than the maximum Ti concentration detected in the blank filters. These filters do not necessarily match the ones used in the homes from which the dust was collected but represent a range of common air filters in the market. The Ti/Nb ratio in the blank filters varied between 126 \pm 77 and 231536 \pm 23715. The Ti/Nb ratio in all blank filters, except the basic pleated, was higher than the natural background Ti/Nb ratio (Fig. S3†), indicating the presence of anthropogenic TiO₂ particles in the blank filters. The high Ti concentrations in the blank filters are most likely due to the use of TiO2 pigment as whitening agent in air filters. Despite the high TiO2 concentrations in some of the blank HVAC filters, their contribution to the dust samples should be limited as we gently scraped the dust samples from the HVAC filter surface and made all possible attempts to minimize the contribution of the HVAC filter material to the dust samples. Thus, we estimate that the majority of the anthropogenic Ti in the dust samples, in particular those collected from homes 7 and 8, is attributed to the dust itself rather than the filter material.

The Ti/Nb ratio in all the home dust samples varies between 227 ± 6 and 5609 ± 1048 . The Ti/Nb ratio in all home dusts, except home dust 4, is higher than the natural background ratio, indicating anthropogenic Ti contamination (Fig. 1b). The anthropogenic Ti concentration was estimated to vary between 0 and 7974 ± 677 mg kg⁻¹ (Fig. 1c). Assuming that anthropogenic Ti is due to pure TiO₂-engineered

particles, the anthropogenic Ti concentration corresponds to 0 to 13 304 \pm 1129 mg TiO₂ kg⁻¹ with the highest concentration in home 8, which was renovated (repainted) prior to sample collection. Therefore, the high TiO2 concentration in home number 8 can be attributed to release of TiO2 from paint sanding, given that TiO2 is most widely used as a pigment in paints.63 This is consistent with previous studies that demonstrated the occurrence of metalbearing particles in home dust.¹⁴ For instance, using micro-X-ray fluorescence and micro-X-ray diffraction approaches, Walker et al. identified Ti-, Pb-, Zn-, Ba-, Cr-, and Cu-bearing particles in home dust and attributed these particles to pigments released from paint during renovation activities because of the presence of lithopone (a mixture of barite and wurtzite), zinc oxide (zincite), hydrocerussite, rutile, and anatase.14 Furthermore, recent trends to incorporate nanosized additives (e.g., SiO2, Fe2O3, SiO2 and TiO2) within concrete (to improve workability and strength) introduce an additional source of engineered particles, which could be released during demolition and recycling.54 Demolition and construction activities associated with building renovation are known to produce substantial amounts of particulate matter (PM), including coarse (PM₁₀ ≤10 µm), fine (PM_{2.5} \leq 2.5 µm), very fine (PM₁ \leq 1 µm), and ultrafine particles (UFP ≤100 nm).64,65 The UFPs were found to account for >90% of the total particle number concentrations and <10% of the total mass concentration released during renovation activities such as wall chasing, drilling, cementing, and general demolition activities.66 The absence of anthropogenic TiO₂ in home dust 4 is ascribed to the fact that this home is located in a remote area and did not undergo any paint or renovation work in the recent years.

3.3. Anthropogenic cerium and lanthanum concentrations

Ce and La concentrations vary from 0.8 ± 0.1 to 16.9 ± 3.7 and 0.4 ± 0.05 to 28.6 ± 6.5 mg kg⁻¹, respectively (Fig. 2). These concentrations are much higher than those detected in the blank filters (Table S4†). The Ce concentrations in the blank filters vary between 0 and 0.1 ± 0.2 mg kg⁻¹.

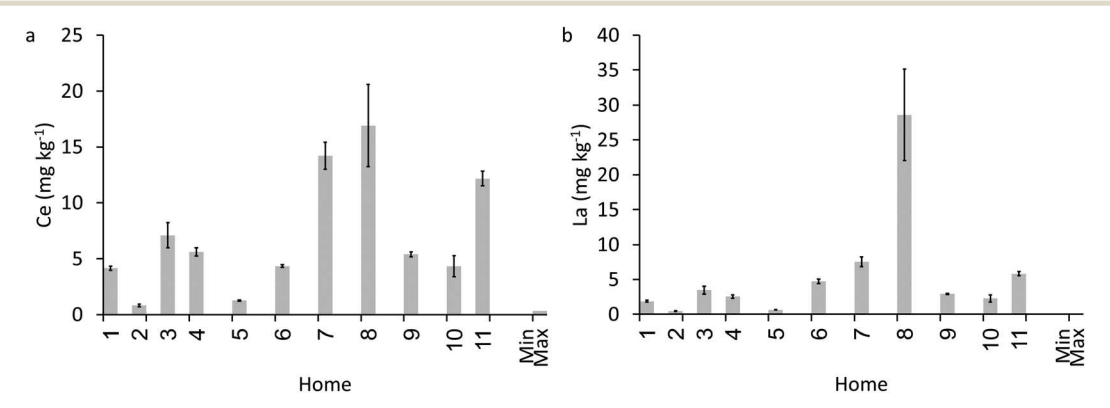


Fig. 2 Concentrations of (a) Ce and (b) La in bulk home dusts collected from the surface of heating, ventilation, and air conditioning (HVAC) units from residential homes. Min and max refer to the minimum and maximum concentrations detected in the five blank HVAC filters.

Lanthanum concentrations in the blank filters are below the ICP-MS limit of detection (0.0096 µg L⁻¹). All dusts, other than those collected from homes 6 and 8, display higher Ce than La concentrations. This gives an initial indication of La contamination in dust 6 and 8, given that Ce is twofold more abundant than La in the upper earth crust.54 Below, we describe how we identified and quantified anthropogenic Ce and La contaminations in the dust samples.

First, we explored the crustal-normalized REE patterns in the dust samples. Crustal-normalized REE concentrations of non-contaminated environmental samples are well known to display a smooth pattern.67,68 Perturbations/spikes in the REE indicate probable normalized profile contamination since the normalization removes the natural variations in absolute concentrations of REEs. From this point of view, spikes in the normalized REE concentration profile can be used as markers of anthropogenic contamination in dust samples. Overall, home dusts are characterized by elevated REE concentrations relative to the upper crustal average concentrations and to the clean filters

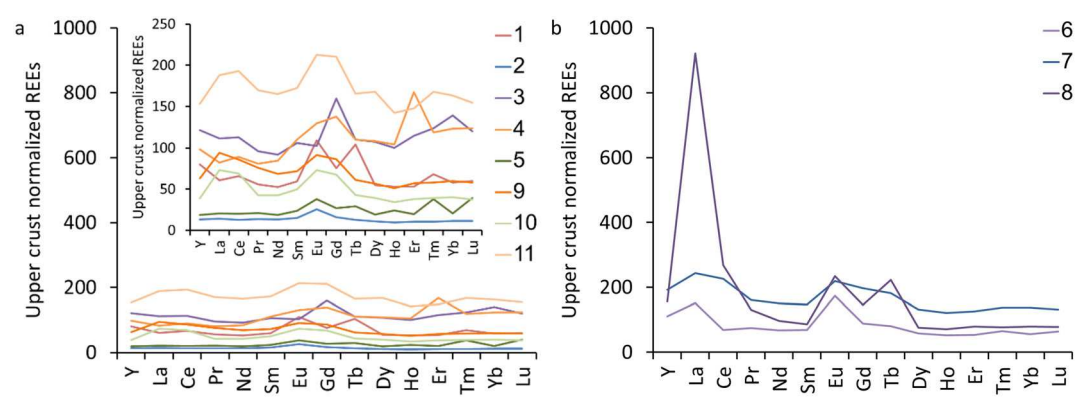


Fig. 3 Upper crust normalized rare earth element concentrations in bulk home dusts collected from the surface of heating, ventilation, and air conditioning (HVAC) units from residential homes: (a) homes 1-5 and 9-11 display a similar pattern to upper average crust and (b) 6-8 show enrichment in Ce and La.

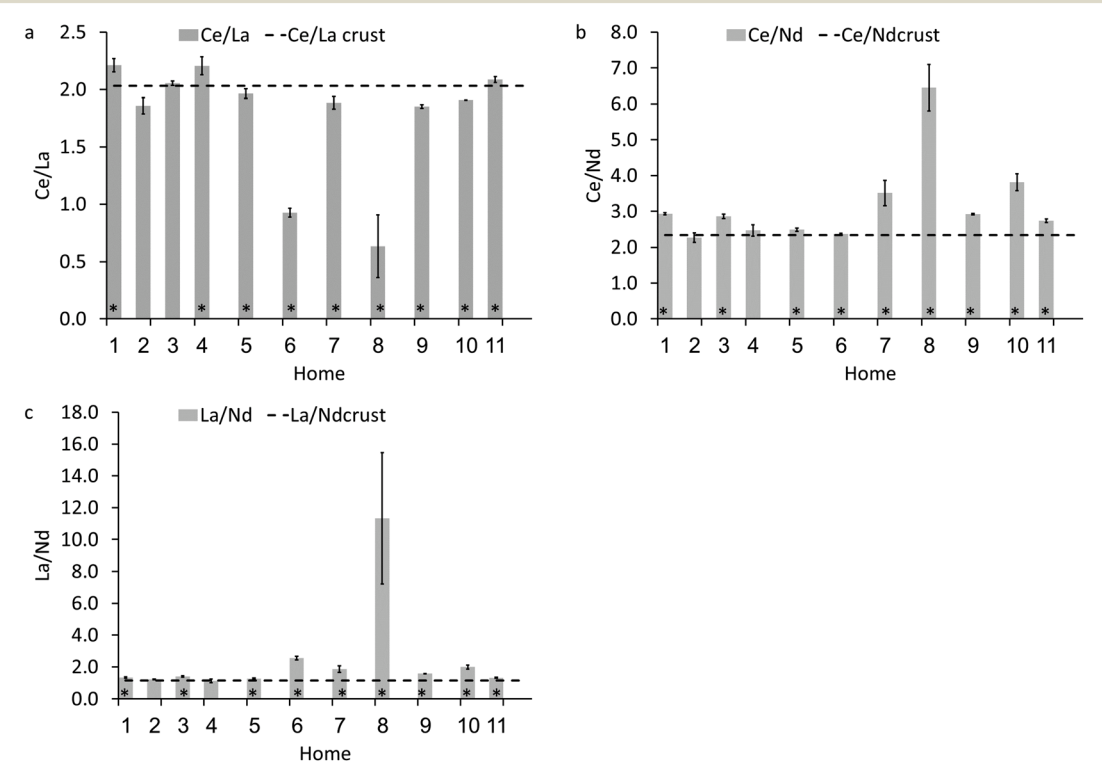


Fig. 4 Elemental ratios of (a) Ce/La, (b) Ce/Nd, and (c) La/Nd in bulk home dusts collected from the surface of heating, ventilation, and air conditioning (HVAC) units from residential homes. * indicates significantly different (t-test) values relative to average crustal Ce/La, Ce/Nd, and La/ Nd ratios

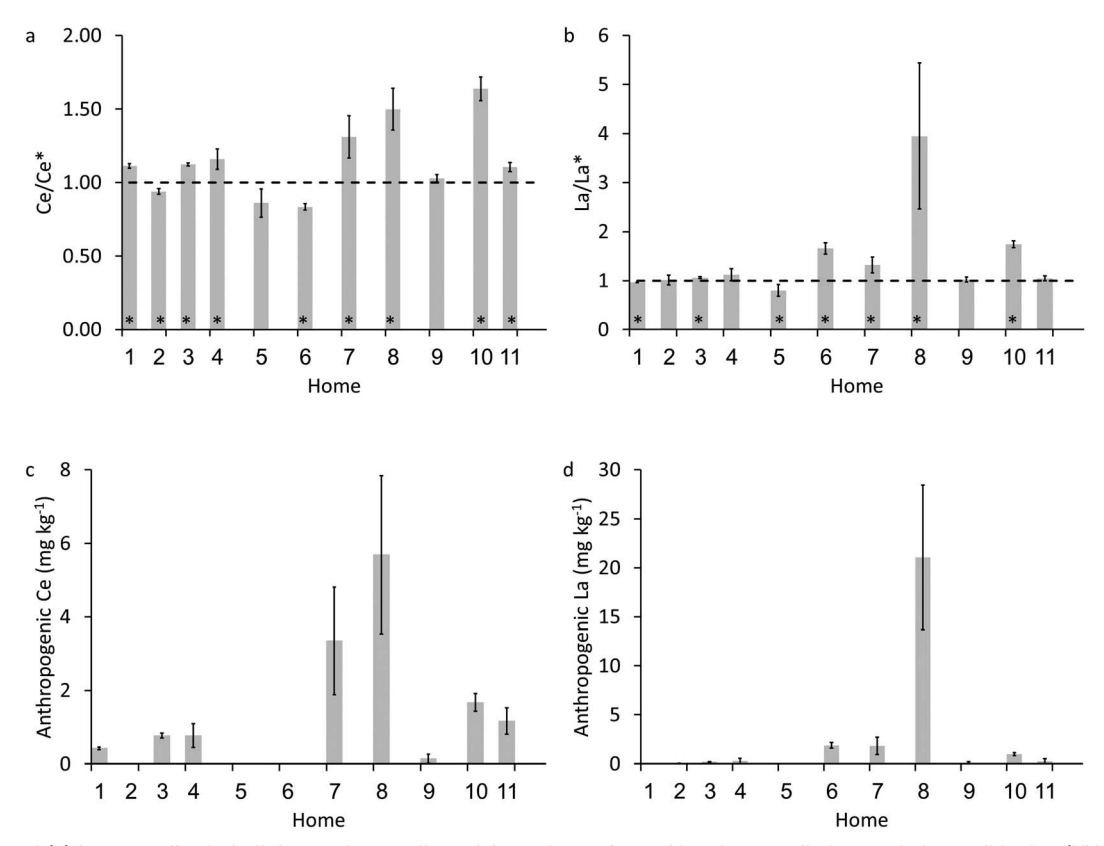
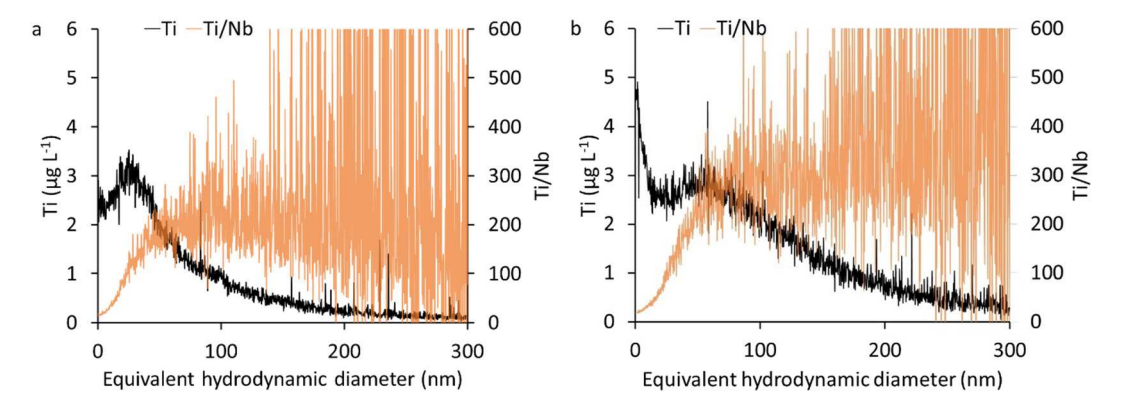


Fig. 5 (a) Ce and (b) La anomalies in bulk home dusts collected from the surface of heating, ventilation, and air conditioning (HVAC) units from residential homes. Concentrations of anthropogenic (c) Ce and (d) La. * indicates significantly different (t-test) values relative to Ce/Ce* and La/ La* of 1.

(Fig. 3 and S4†). The overall patterns of the upper crustalnormalized REEs in dusts from homes 1-5 and 9-11 are uniform and display a similar pattern to that of the upper average crust (Fig. 3a), indicating that the REEs in these dusts originate from natural sources. In contrast, the upper crustal-normalized REE profile in dust samples from homes 6-8 shows enrichment in Ce and La (Fig. 3b), with the dust from home 8 showing the highest enrichment in Ce and La, indicating that dust from these homes originates from a mix of natural and anthropogenic sources. In particular, the pattern of upper crustal-normalized REEs in dust 8 is strongly perturbed.

Elemental ratios of Ce to La in the bulk dust samples varied from 0.6 to 2.2, indicating possible Ce and La contamination in home dusts (Fig. 4a). More specifically, Ce/La in dusts collected from homes 1 and 4 have slightly higher elemental ratios than the upper crustal value (i.e., 2.0), suggesting that dust from these homes might potentially be contaminated with Ce. Additionally, Ce/La in dusts from homes 2 and 6-10 have lower ratios compared to the upper crustal value, with the lowest ratios in dusts from homes 6 and 8, suggesting that dusts from these homes are potentially contaminated with La. Given that the dust samples might be contaminated with both Ce and La and that Nd (the next most abundant REE after Ce and La) does not seem to be enriched in any of the dust samples (Fig. 3), we calculated the elemental ratios of Ce/Nd and La/Nd (Fig. 4b and c). The elemental ratios of Ce/Nd (Fig. 4b) indicate that dust from homes 1, 3 and 7-11 has higher values than the average crustal value (i.e., 2.33), with the highest Ce/Nd ratio of 6.5 measured in home dust 8, indicating that dusts from these homes are potentially contaminated with Ce. The La/Nd ratio (Fig. 4c) indicates that dust from homes 6-10 has higher values than the average crustal value (i.e., 1.15), with the highest La/Nd ratio of 11.3 measured in home dust 8, indicating that dusts from these homes are potentially contaminated with La. The dust from home 8 exhibited the lowest Ce/La and the highest Ce/Nd and La/Nd ratios, indicating that this dust is most likely contaminated with both Ce and La.

An alternative approach to elemental ratio analysis is based on calculating the size of REE anomalies in order to identify and quantify anthropogenic REE concentrations.⁵⁶ The size of Ce and La anomalies (Ce/Ce* and La/La*, Fig. 5a and b) varies from 0.8 to 1.64 and 0.8 to 3.95, indicating that several home dusts are contaminated with Ce and La. The sizes of Ce anomalies are <1.5 for all dusts except dust from homes 8 and 10, for which Ce anomalies are 1.5 and 1.64, respectively, indicating potential contamination with Ce in these two homes. The sizes of La anomalies are <1.5 in all dust samples except dust from homes 6, 8 and 10, for which La anomalies are 1.66, 3.95, and 1.74, respectively, indicating that dust from homes 6, 8 and 10 is contaminated with La. The estimated anthropogenic Ce and La concentrations



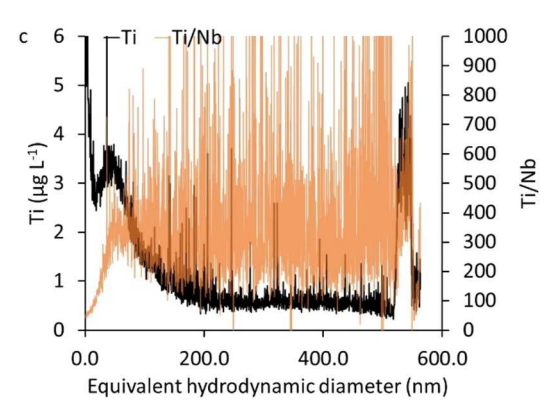


Fig. 6 Size-based Ti concentration and Ti/Nb elemental ratio distributions in the <450 nm extracted particle fractions from dusts collected from homes (a) 4, (b) 7, and (c) 8. Particles were fractionated using asymmetrical flow-field flow fractionation (AF4) and metals were analyzed by inductively coupled plasma-mass spectrometry (ICP-MS).

vary between 0 and 5.7 \pm 2.2 mg Ce kg⁻¹ and 0 and 21.1 \pm 7.4 mg La kg⁻¹, respectively (Fig. 5c and d).

The high Ce and La concentrations in dust 8 are likely due to indoor emissions during the house renovation such as paint pigments and/or driers. La₂O₃ is used as a pigment in paint. Additionally, driers used in solvent-based and waterbased paints containing unsaturated polymers are principally metal salts (lead, calcium, cobalt, manganese, cerium, and lanthanum) of naphthenic acid and neodecanoic acid. 69,70 Other uses of Ce and La within the indoor environment that could result in their release include the use of cerium as the major component of mischmetal alloy (just under 50%) which is used in 'flints' for lighters; Ce2O3 as a catalyst in the inside walls of self-cleaning ovens to prevent the build-up of cooking residues; cerium in flat-screen TVs and low-energy light bulbs in the indoor environment;71,72 and La in equipment such as color televisions, fluorescent lamps, and energy-saving lamps and glasses.^{72,73}

3.4. Elemental size-based distribution

Particles <0.45 µm were extracted from dust with the lowest (home 4), intermediate (home 7), and highest (home 8) Ti/Nb ratio and were analyzed by AF4-ICP-MS to determine their size-based elemental concentrations and ratio distributions (raw AF4-ICP-MS data are presented in Fig. S5†). The Ti/Nb ratios are approximately 300 in <0.45 µm fractions for all dust samples (Fig. 6), similar to those reported in noncontaminated soil particles, 31,51 indicating the absence of anthropogenic TiO2 particles in the extracted suspensions. Thus, the high Ti/Nb ratio in the bulk dust samples can be attributed to the contamination of the dust samples with large or heteroaggregated Ti-bearing particles. The high variability in Ti/Nb elemental ratios likely reflects low Nb concentrations (close to the limit of quantification) as it occurs at low concentrations in natural Ti-bearing minerals.

The elemental size distribution of Ce and La in the <0.45 µm suspensions extracted from dusts from homes 4, 7 and 8 (no, low, and high La contamination) is presented in Fig. 7 and shows that Ce and La co-eluted in the size range of 1 to 100 nm. The Ce/La ratios in dusts 4 and 7 vary between 1 and 2, whereas those in dust 8 vary between 0.05 and 0.2. These results follow the same trend as the elemental ratios calculated on the bulk dust samples (Fig. 4a). Furthermore, the elemental ratios of Ce/Nd and La/Nd are presented in Fig. 8. The extracted suspensions exhibit Ce/Nd ratios close to the average crustal values (Fig. 8a, c and e), whereas the elemental ratio of La/Nd exhibits higher values than the

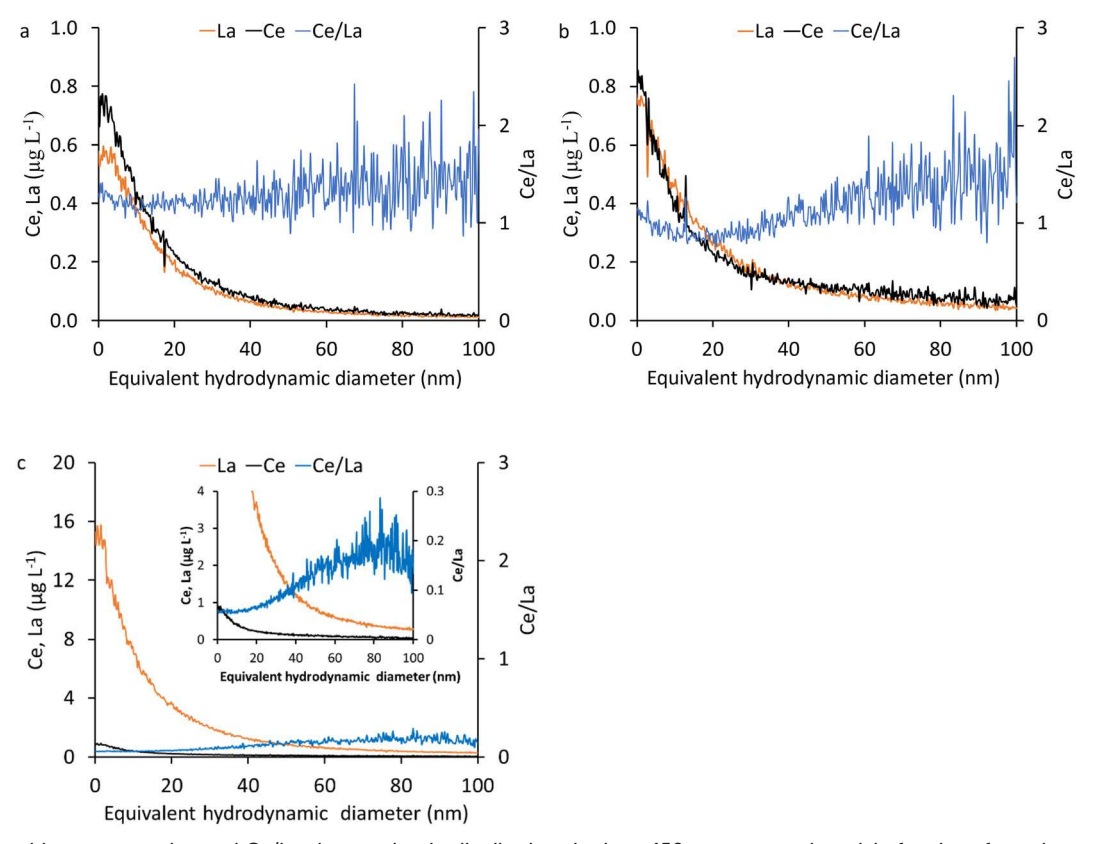


Fig. 7 Size-based La concentration and Ce/La elemental ratio distributions in the <450 nm extracted particle fractions from dusts collected from homes (a) 4, (b) 7, and (c) 8. Particles were fractionated using asymmetrical flow-field flow fractionation (AF4) and metals were analyzed by inductively coupled plasma-mass spectrometry (ICP-MS).

average crustal values in all dusts, with slightly higher ratios in dusts from homes 4 and 7 (Fig. 8b and d) and much higher ratios in dust from home 8 (Fig. 8c), in good agreement with the bulk elemental ratio trends (Fig. 4c). These results indicate that there is no or low Ce contamination in all home dust samples, no or low La contamination in dust 4 and 7, and high La contamination in dust 8.

Whereas anthropogenic Ti occurs as large particles >450 nm, anthropogenic La-bearing particles occur as nano-sized particles (e.g., <60 nm, Fig. 7 and 8). These differences might be attributed to the different sources of Ti and La or to the differences in the release of Ti and La from the same source. The likely source of anthropogenic Ti and La in dust 8 was the paint used during renovation. TiO2 (100-300 nm) is the most widely used pigment in paints. Additionally, the use of 0.5-5% (w/w) nanomaterials (10-100 nm, including La₂O₃) remarkably improves the properties of paint in terms of scratch resistance, hardness, gloss, weather stability, and cross-linking and hardening properties.⁷⁰ Nanomaterials and pigments are present as single particles in paint only at the time of manufacturing. They increase in effective size by agglomeration and by absorption of polymers and surfaceactive agents onto their surface. During the drying process, the particles continue to agglomerate and are incorporated irreversibly into the polymer matrix.⁷⁰ It is worth noting that

gray/white chunks were visually observed in the settled particles during the separation of the <450 nm size fraction, and qualitatively smaller quantities of these gray/white chunks were observed in dust 7 sediment. Thus, most likely TiO₂ particles were released as a component of paint fragments. In contrast, La2O3 particles were likely released as smaller aggregates/primary particles. The release of small Labearing particles could also be attributed to the fact that surface functionalized La2O3 nanomaterials, using chemically bound polymers, allow for the La2O3 nanomaterials to be preferentially adsorbed at the surface interface in solventbased and water-based paints.74

4. Conclusions and environmental implications

This study investigated the occurrence of anthropogenic Ti, Ce, and La in eleven home dusts collected from surface HVAC filters in Columbia, South Carolina, USA. To the best of our knowledge, this study provides the first dataset on anthropogenic Ti-, Ce-, and La-bearing concentrations in home dusts. The concentration of anthropogenic titanium, cerium, and lanthanum varied between 0 to 8000 mg Ti kg⁻¹, 0 to 6 mg Ce kg⁻¹, and 0 to 21 mg La kg⁻¹, respectively. Whereas anthropogenic Ti-bearing particles occurred as large particles >450 nm, anthropogenic

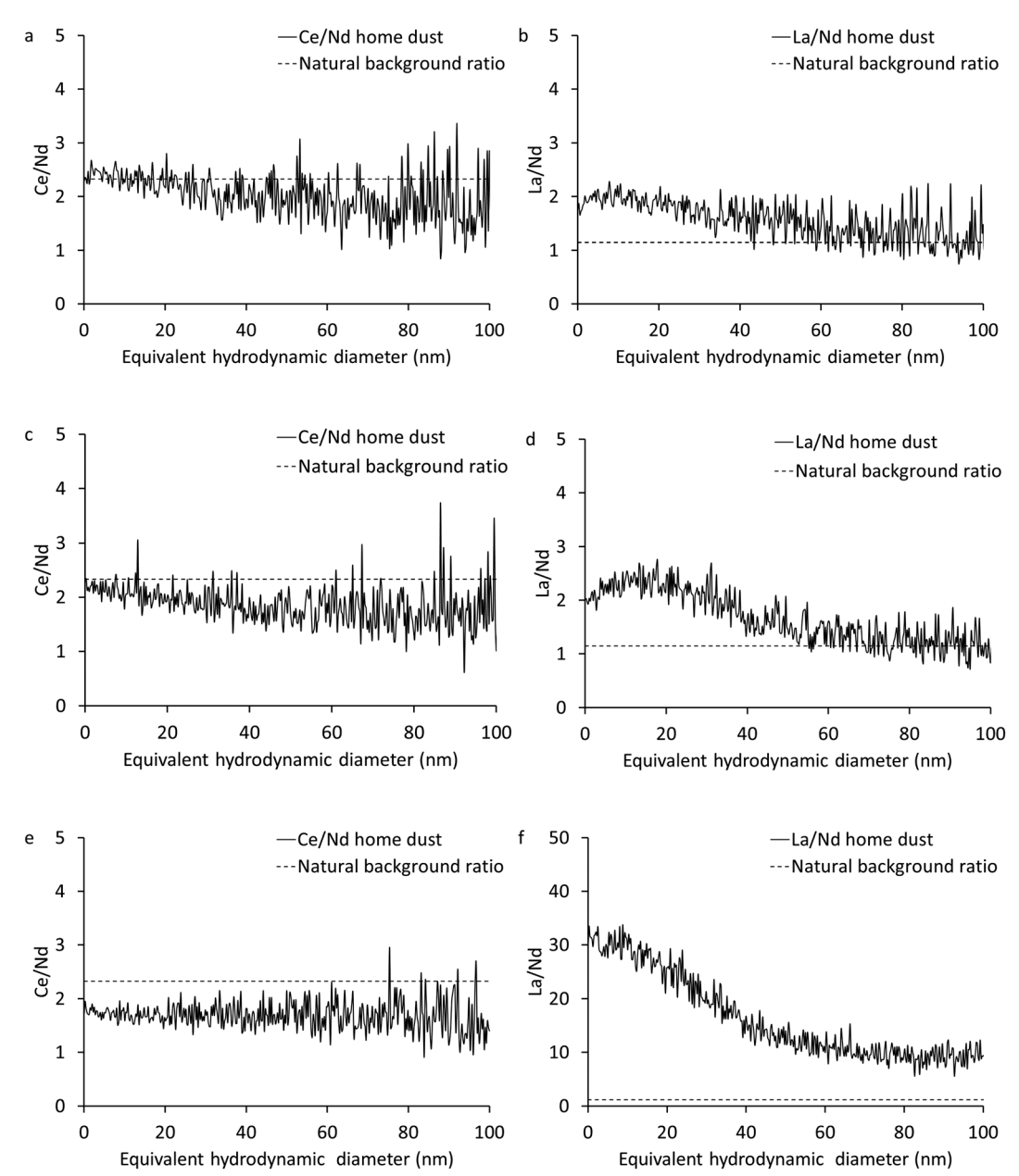


Fig. 8 Size-based elemental ratios of (a, c and e) Ce/Nd and (b, d and f) La/Nd in the extracted <450 nm particle fractions from dusts collected from homes (a and b) 4, (c and d) 7, and (f and e) 8. Particles were fractionated using asymmetrical flow-field flow fractionation (AF4) and metals were analyzed by inductively coupled plasma-mass spectrometry (ICP-MS).

La-bearing particles occurred in the nanosized range. These differences in anthropogenic particle size could be attributed to the size of the particles used or to the nature of the released particles. The occurrence of these anthropogenic particles (likely as TiO₂, CeO₂ and La₂O₃) in home dust implies that these particles were suspended in indoor air and thus are available for inhalation and for transport to eating and food preparation areas. The high anthropogenic Ti and La concentrations (likely as TiO₂ and La₂O₃) in the renovated home dust imply the exposure of construction workers to high levels of these particles. Such a high level of exposure is a potential hazard to human health. For instance, TiO₂

particles are likely to cause diseases in humans, including tumors and cancer, and affect the brain, heart, intestinal mucosa, and other internal organs. TiO₂ particles are classified as suspected carcinogens to humans by inhalation. Additionally, the use of TiO₂ as a food additive has been recently banned by the European Union due to potential human health implications. Reports on indoor air concentrations of Ce and La and their related health effects are scarce. Nonetheless, occupational exposure to CeO₂ and La₂O₃ nanomaterials has been shown to result in the accumulation of cerium in the lungs and to cause lung diseases such as pneumoconiosis, endomyocardial fibrosis,

and myocardial infarction.^{77–85} Overall, the presence of these particles in home dusts may pose indoor environment air quality and human health risks due to elongated and continuous exposure.

The findings of this study also have significant implications for the detection and quantification of engineered nanomaterials (e.g., CeO₂ and La₂O₃) in environmental samples. For instance, the increases in the elemental ratios of Ce/La above the natural background ratios have been suggested as a proxy for the detection and quantification of CeO₂ NMs in environmental samples. However, the co-contamination of samples with both Ce and La may lead to erroneous results. In such a scenario, the use of alternative ratios such as Ce/Nd, La/Nd and Ce and La anomaly analysis provides an alternative tool to the elemental ratio of Ce to La.

Author contributions

Dr. Mohammed Baalousha conceived the overall idea of the research and coordinated sample collection. Mr. MD Mahmudun Nabi and Dr. Jingjing Wang performed all experimental work and data analysis. Mr. MD Mahmudun Nabi wrote the first draft. All authors contributed to the manuscript writing and editing.

Conflicts of interest

The authors declare no competing interest.

Acknowledgements

This work was supported by a US National Science Foundation CAREER (1553909) grant to Dr. Mohammed Baalousha.

References

- 1 P. B. Kurt-Karakus, Determination of heavy metals in indoor dust from Istanbul, Turkey: Estimation of the health risk, *Environ. Int.*, 2012, **50**, 47–55.
- 2 P. E. Rasmussen, et al., Canadian House Dust Study: Population-based concentrations, loads and loading rates of arsenic, cadmium, chromium, copper, nickel, lead, and zinc inside urban homes, Sci. Total Environ., 2013, 443, 520–529.
- 3 J. Yoshinaga, *et al.*, Lead and other elements in house dust of Japanese residences Source of lead and health risks due to metal exposure, *Environ. Pollut.*, 2014, **189**, 223–228.
- 4 J. A. Leech, W. C. Nelson, R. T. Burnett, S. Aaron and M. E. Raizenne, It's about time: A comparison of Canadian and American time-activity patterns, *J. Exposure Sci. Environ. Epidemiol.*, 2002, **12**, 427–432.
- 5 S. Brasche and W. Bischof, Daily time spent indoors in German homes Baseline data for the assessment of indoor exposure of German occupants, *Int. J. Hyg. Environ. Health*, 2005, **208**, 247–253.
- 6 I. N. Y. Doyi, C. F. Isley, N. S. Soltani and M. P. Taylor, Human exposure and risk associated with trace element

- concentrations in indoor dust from Australian homes, *Environ. Int.*, 2019, **133**, 105125.
- 7 T. Whitehead, C. Metayer, P. Buffler and S. M. Rappaport, Estimating exposures to indoor contaminants using residential dust, J. Exposure Sci. Environ. Epidemiol., 2011, 21, 549–564.
- 8 M. S. Waring, Secondary organic aerosol in residences: predicting its fraction of fine particle mass and determinants of formation strength, *Indoor Air*, 2014, 24, 376–389.
- 9 M. S. Waring and J. A. Siegel, An evaluation of the indoor air quality in bars before and after a smoking ban in Austin, Texas, *J. Exposure Sci. Environ. Epidemiol.*, 2006, 17, 260–268.
- 10 T. Schripp, D. Markewitz, E. Uhde and T. Salthammer, Does e-cigarette consumption cause passive vaping?, *Indoor Air*, 2013, 23, 25–31.
- 11 L. Wallace, Indoor Sources of Ultrafine and Accumulation Mode Particles: Size Distributions, Size-Resolved Concentrations, and Source Strengths, *Aerosol Sci. Technol.*, 2006, 40, 348–360.
- 12 L. Wallace, Indoor Particles: A Review, *J. Air Waste Manage.* Assoc., 1996, **46**, 98–126.
- 13 A. A. Abdel Hameed, I. H. Yasser and I. M. Khoder, Indoor air quality during renovation actions: a case study, *J. Environ. Monit.*, 2004, **6**, 740–744.
- 14 S. R. Walker, H. E. Jamieson and P. E. Rasmussen, Application of Synchrotron Microprobe Methods to Solid-Phase Speciation of Metals and Metalloids in House Dust, *Environ. Sci. Technol.*, 2011, 45, 8233–8240.
- 15 C. A. Belis, F. Karagulian, B. R. Larsen and P. K. Hopke, Critical review and meta-analysis of ambient particulate matter source apportionment using receptor models in Europe, Atmos. Environ., 2013, 69, 94–108.
- 16 P. E. Rasmussen, C. Levesque, M. Chénier and H. D. Gardner, Contribution of metals in resuspended dust to indoor and personal inhalation exposures: Relationships between PM10 and settled dust, *Build. Environ.*, 2018, 143, 513–522.
- 17 T. L. Conner, G. A. Norris, M. S. Landis and R. W. Williams, Individual particle analysis of indoor, outdoor, and community samples from the 1998 Baltimore particulate matter study, *Atmos. Environ.*, 2001, 35, 3935–3946.
- 18 L. Calderón, et al., Release of airborne particles and Ag and Zn compounds from nanotechnology-enabled consumer sprays: Implications for inhalation exposure, Atmos. Environ., 2017, 155, 85–96.
- 19 M. A. Bari, *et al.*, Indoor and Outdoor Levels and Sources of Submicron Particles (PM1) at Homes in Edmonton, Canada, *Environ. Sci. Technol.*, 2015, **49**, 6419–6429.
- 20 S. Suryawanshi, A. S. Chauhan, R. Verma and T. Gupta, Identification and quantification of indoor air pollutant sources within a residential academic campus, *Sci. Total Environ.*, 2016, 569–570, 46–52.
- 21 P. E. Rasmussen, *et al.*, Impact of humidity on speciation and bioaccessibility of Pb, Zn, Co and Se in house dust, *J. Anal. At. Spectrom.*, 2014, **29**, 1206–1217.
- 22 L. C. W. MacLean, S. Beauchemin and P. E. Rasmussen, Lead Speciation in House Dust from Canadian Urban Homes Using EXAFS, Micro-XRF, and Micro-XRD, *Environ. Sci. Technol.*, 2011, 45, 5491–5497.

- 23 S. Beauchemin, P. E. Rasmussen, T. MacKinnon, M. Chénier and K. Boros, Zinc in House Dust: Speciation, Bioaccessibility, and Impact of Humidity, Environ. Sci. Technol., 2014, 48, 9022-9029.
- 24 S. Beauchemin, L. C. W. MacLean and P. E. Rasmussen, Lead speciation in indoor dust: a case study to assess old paint contribution in a Canadian urban house, Environ. Geochem. Health, 2011, 33, 343-352.
- 25 F. von der Kammer, P. L. Ferguson, P. A. Holden, A. Masion, K. R. Rogers, S. J. Klaine, A. A. Koelmans, N. Horne and J. M. Unrine, et al., Analysis of engineered nanomaterials in complex matrices (environment and biota): general considerations and conceptual case studies, Environ. Toxicol. Chem., 2012, 31, 32-49.
- 26 European Union Regulation Commission, Amending Annexes II and III to Regulation (EC) No 1333/2008 of the European Parliament and of the Council as regards the food additive titanium dioxide (E 171), 2022.
- 27 M. D. Montaño, et al., Current status and future direction for examining engineered nanoparticles in natural systems, Environ. Chem., 2014, 11, 351-366.
- 28 D. L. Slomberg, et al., Anthropogenic Release and Distribution of Titanium Dioxide Particles in a River Downstream of a Nanomaterial Manufacturer Industrial Site, Front. Environ. Sci., 2020, 76.
- 29 K. Mehrabi, R. Kaegi, D. Günther and A. Gundlach-Graham, Emerging investigator series: automated single-nanoparticle quantification and classification: a holistic study of particles into and out of wastewater treatment plants in Switzerland, Environ. Sci.: Nano, 2021, 8, 1211-1225.
- 30 Y. Morera-Gómez, J. M. Santamaría, D. Elustondo, E. Lasheras and C. M. Alonso-Hernández, Determination and source apportionment of major and trace elements in atmospheric bulk deposition in a Caribbean rural area, Atmos. Environ., 2019, 202, 93-104.
- 31 Z. Yi, F. Loosli, J. Wang, D. Berti and M. Baalousha, How to distinguish natural versus engineered nanomaterials: insights from the analysis of TiO2 and CeO2 in soils, Environ. Chem. Lett., 2020, 18, 215-227.
- 32 F. Loosli, et al., Sewage spills are a major source of titanium dioxide engineered (nano)-particle release into the environment, Environ. Sci.: Nano, 2019, 6, 763-777.
- 33 M. M. Nabi, J. Wang and M. Baalousha, Episodic surges in titanium dioxide engineered particle concentrations in surface waters following rainfall events, Chemosphere, 2021, 263, 128261.
- 34 J. Wang, et al., Detection and quantification of engineered particles in urban runoff, Chemosphere, 2020, 248, 126070.
- 35 M. Baalousha, J. Wang, M. Erfani and E. Goharian, Elemental fingerprints in natural nanomaterials determined using SP-ICP-TOF-MS and clustering analysis, Sci. Total Environ., 2021, 792, 148426.
- 36 M. M. Nabi, J. Wang, C. A. Journey, P. M. Bradley and M. Baalousha, Temporal variability in TiO2 engineered particle concentrations in rural Edisto River, Chemosphere, 2022, 297, 134091.

- 37 T. Feiyun, et al., Multi-method approach for analysis of road dust particles: elemental ratios, SP-ICP-TOF-MS, and TEM, Environ. Sci.: Nano, 2022, 12, 2022.
- 38 M. Baalousha, et al., Stormwater green infrastructures retain high concentrations of TiO2 engineered (nano)-particles, I. Hazard. Mater., 2020, 392, 122335.
- 39 O. Meili-Borovinskaya, et al., Analysis of complex particle mixtures by asymmetrical flow field-flow fractionation coupled to inductively coupled plasma time-of-flight mass spectrometry, J. Chromatogr. A, 1641, 2021, 461981.
- M. Baalousha, J. Wang, M. Erfani and E. Goharian, Elemental fingerprints in natural nanomaterials determined using SP-ICP-TOF-MS and clustering analysis, Sci. Total Environ., 2021, 792, 148426.
- 41 A. Gondikas, et al., Where is the nano? Analytical approaches for the detection and quantification of TiO 2 engineered nanoparticles in surface waters, Environ. Sci.: Nano, 2018, 5, 313-326.
- Praetorius, et al., Single-particle multi-element 42 A. fingerprinting (spMEF) using inductively-coupled plasma time-of-flight mass spectrometry (ICP-TOFMS) to identify engineered nanoparticles against the elevated natural background in soils, Environ. Sci.: Nano, 2017, 4, 307-314.
- 43 A. Gundlach-Graham, Multiplexed and multi-metal singleparticle characterization with ICP-TOFMS, Compr. Anal. Chem., 2021, 93, 69-101.
- 44 R. Kaegi, et al., Release of TiO 2 (Nano) particles from construction and demolition landfills, NanoImpact, 2017, 8,
- 45 S. Lee, et al., Nanoparticle size detection limits by single particle ICP-MS for 40 elements, Environ. Sci. Technol., 2014, 48, 10291-10300.
- 46 M. Baalousha, J. Wang, M. Erfani and E. Goharian, Elemental fingerprints in natural nanomaterials determined using SP-ICP-TOF-MS and clustering analysis, Sci. Total Environ., 2021, 792, 148426.
- 47 M. Baalousha, et al., Characterization of cerium oxide nanoparticles-Part 1: Size measurements, Environ. Toxicol. Chem., 2012, 31, 983-993.
- 48 M. Baalousha, et al., Characterization of cerium oxide nanoparticles-Part 2: Nonsize measurements, Environ. Toxicol. Chem., 2012, 31, 994-1003.
- J. A. Oppenheimer, M. Badruzzaman and J. G. Jacangelo, Differentiating sources of anthropogenic loading to impaired water bodies utilizing ratios of sucralose and other microconstituents, Water Res., 2012, 46, 5904-5916.
- 50 A. Knappe, P. Möller, P. Dulski and A. Pekdeger, Positive gadolinium anomaly in surface water and ground water of the urban area Berlin, Germany, Geochemistry, 2005, 65, 167-189.
- F. Loosli, Z. Yi, J. Wang and M. Baalousha, Improved extraction efficiency of natural nanomaterials in soils to facilitate their characterization using a multimethod approach, Sci. Total Environ., 2019, 677, 34-46.
- 52 A. J. Bednar, et al., Comparison of on-line detectors for field flow fractionation analysis of nanomaterials, Talanta, 2013, 104, 140-148.

- 53 R. Saenmuangchin and A. Siripinyanond, Flow field-flow fractionation for hydrodynamic diameter estimation of gold nanoparticles with various types of surface coatings, *Anal. Bioanal. Chem.*, 2018, **410**, 6845–6859.
- 54 R. L. Rudnick and D. M. Fountain, Nature and composition of the continental crust: A lower crustal perspective, *Rev. Geophys.*, 1995, 33, 267.
- 55 M. G. Lawrence, A. Greig, K. D. Collerson and B. S. Kamber, Rare Earth Element and Yttrium Variability in South East Queensland Waterways, *Aquat. Geochem.*, 2006, **12**, 39–72.
- 56 M. G. Lawrence, C. Ort and J. Keller, Detection of anthropogenic gadolinium in treated wastewater in South East Queensland, Australia, Water Res., 2009, 43, 3534–3540.
- 57 A. Hunt, D. L. Johnson and D. A. Griffith, Mass transfer of soil indoors by track-in on footwear, *Sci. Total Environ.*, 2006, 370, 360–371.
- 58 P. E. Rasmussen, K. S. Subramanian and B. J. Jessiman, A multi-element profile of house dust in relation to exterior dust and soils in the city of Ottawa, Canada, *Sci. Total Environ.*, 2001, 267, 125–140.
- 59 W. Butte and B. Heinzow, Pollutants in house dust as indicators of indoor contamination, *Rev. Environ. Contam. Toxicol.*, 2002, 175, 1–46.
- 60 C. Lanzerstorfer, Variations in the composition of house dust by particle size, *J. Environ. Sci. Health, Part A: Toxic/Hazard. Subst. Environ. Eng.*, 2017, 52, 770–777.
- 61 J. E. Fergusson, E. A. Forbes, R. J. Schroeder and D. E. Ryan, The elemental composition and sources of house dust and street dust, *Sci. Total Environ.*, 1986, **50**, 217–221.
- 62 E. Y. Wang, R. D. Willis, T. J. Buckley, G. G. Rhoads and P. J. Lioy, The Relationship Between the Dust Lead Concentration and the Particle Sizes of Household Dusts Collected in Jersey City Residences, *Appl. Occup. Environ. Hyg.*, 2011, 11, 199–206.
- 63 J. H. Braun, A. Baidins and R. E. Marganski, TiO2 pigment technology: a review, *Prog. Org. Coat.*, 1992, **20**, 105–138.
- 64 P. Kumar, M. Mulheron, B. Fisher and R. M. Harrison, New Directions: Airborne ultrafine particle dust from building activities – A source in need of quantification, *Atmos. Environ.*, 2012, 56, 262–264.
- P. Kumar, L. Pirjola, M. Ketzel and R. M. Harrison,
 Nanoparticle emissions from 11 non-vehicle exhaust sources
 A review, Atmos. Environ., 2013, 67, 252–277.
- 66 F. Azarmi, et al., Physicochemical characteristics and occupational exposure to coarse, fine and ultrafine particles during building refurbishment activities, J. Nanopart. Res., 2015, 17, 1–19.
- 67 S. Kulaksiz and M. Bau, Contrasting behaviour of anthropogenic gadolinium and natural rare earth elements in estuaries and the gadolinium input into the North Sea, *Earth Planet. Sci. Lett.*, 2007, **260**, 361–371.
- 68 M. G. Lawrence, *et al.*, Aquatic geochemistry of the rare earth elements and yttrium in the Pioneer River catchment, Australia, *Mar. Freshwater Res.*, 2006, 57, 725–736.
- 69 T. Brock, M. Groteklaes and P. Mischke, European Coatings Handbook, Eur. Coatings Handb., 2019, DOI: 10.1515/ 9783748602255/HTML.

- 70 International Agency for Research on Cancer, Working Group on the Evaluation of Carcinogenic Risks To Humans, Chemical Agents and Related Occupations International Agency for Research on Cancer Monographs on the Evaluation of Carcinogenic Risks to Humans, IARC, Lyon, France, 2012.
- 71 J. Chen, Y. Xiao, B. Huang and X. Sun, Sustainable cool pigments based on iron and tungsten co-doped lanthanum cerium oxide with high NIR reflectance for energy saving, *Dyes Pigm.*, 2018, 154, 1–7.
- 72 A. Böhlandt, *et al.*, High concentrations of cadmium, cerium and lanthanum in indoor air due to environmental tobacco smoke, *Sci. Total Environ.*, 2012, **414**, 738–741.
- 73 K. Binnemans, P. T. Jones, T. Müller and L. Yurramendi, Rare Earths and the Balance Problem: How to Deal with Changing Markets?, J. Sustain. Metall., 2018, 4, 126–146.
- 74 American elements, Lanthanum Nanoparticles | AMERICAN ELEMENTS ® | CAS 7439-91-0, Available at: https://www.americanelements.com/lanthanum-nanoparticles-7439-91-0, (Accessed: 10th September 2021).
- 75 E. Baranowska-Wójcik, D. Szwajgier, P. Oleszczuk and A. Winiarska-Mieczan, Effects of Titanium Dioxide Nanoparticles Exposure on Human Health—a Review, *Biol. Trace Elem. Res.*, 2019, 193, 118–129.
- 76 J. L. Adgate, *et al.*, Relationships between personal, indoor, and outdoor exposures to trace elements in PM2.5, *Sci. Total Environ.*, 2007, 386, 21–32.
- 77 L. Kuruvilla and C. Cheranellore Kartha, Cerium depresses endocardial endothelial cell-mediated proliferation of cardiac fibroblasts, *Biol. Trace Elem. Res.*, 2006, **114**, 85–92.
- 78 J. Gómez-Aracena, et al., Toenail cerium levels and risk of a first acute myocardial infarction: The EURAMIC and heavy metals study, Chemosphere, 2006, 64, 112–120.
- 79 I. S. Kim, M. Baek and S. J. Choi, Comparative Cytotoxicity of Al 2O 3, CeO 2, TiO 2and ZnO nanoparticles to human lung cells, J. Nanosci. Nanotechnol., 2010, 10, 3453–3458.
- 80 F. R. Cassee, *et al.*, Exposure, Health and Ecological Effects Review of Engineered Nanoscale Cerium and Cerium Oxide Associated with its Use as a Fuel Additive, *Crit. Rev. Toxicol.*, 2011, 41, 213–229.
- 81 G. Vocaturo, *et al.*, Human Exposure to Heavy Metals: Rare Earth Pneumoconiosis in Occupational Workers, *Chest*, 1983, **83**, 780–783.
- 82 M. Ahamed, M. J. Akhtar, M. A. Majeed Khan, Z. M. Alaizeri and H. A. Alhadlaq, Evaluation of the Cytotoxicity and Oxidative Stress Response of CeO 2-RGO Nanocomposites in Human Lung Epithelial A549 Cells, *Nanomaterials*, 2019, 9(12), 1709.
- 83 J. D. Sisler, et al., Toxicological Assessment of CoO and La2O3 Metal Oxide Nanoparticles in Human Small Airway Epithelial Cells, Toxicol. Sci., 2016, 150, 418–428.
- 84 C. H. Lim, Toxicity of Two Different Sized Lanthanum Oxides in Cultured Cells and Sprague-Dawley Rats, *Toxicol. Res.*, 2015, **31**, 181–189.
- 85 US EPA, Toxicological review of Cerium Oxide and Cerium Compounds. In Support of Summary Information on the Integrated Risk Information System (IRIS), 2009.